Photoelectric Characterization of Forward Electron Transfer to Iron−Sulfur Centers in Photosystem I

Winfried Leibl,* Bruno Toupance, and Jacques Breton

CEA-Saclay, Section de Bioénergétique, Département de Biologie Cellulaire et Moléculaire, 91191 Gif-sur-Yvette, France

Received December 29, 1994; Revised Manuscript Received April 3, 1995[⊗]

ABSTRACT: The photoelectric response of oriented PS I membranes from the cyanobacterium *Synechocystis* 6803 has been investigated in the nanosecond time range. Besides an unresolved rapidly rising phase, there is a further positive electrogenic phase with a rise time constant of 220 ± 20 ns. The amplitude of the 220-ns phase is 66 ± 10% that of the subnanosecond phase. The fast phase contains two kinetic components faster than 100 ps, which have recently been resolved and attributed to primary charge separation ($P^+A_0^-$ formation) and subsequent electron transfer to A_1, respectively (Hecks, B., Wulf, K., Breton, J., Leibl, W., & Trissl, H.-W. (1994) *Biochemistry 33*, 8619−8624). The 220-ns phase is lost under conditions where iron−sulfur centers F_A, F_B, and F_X are prereduced, and its kinetics match the reoxidation kinetics of A_1^- as verified by absorbance change measurements at 380 nm. Therefore, this electrogenic phase is attributed to electron transfer to the iron−sulfur centers that function as further electron acceptors in the PS I reaction center. Gradual removal of F_A and F_B by urea treatment reveals that the amplitude of the 220-ns phase is linearly correlated with the fraction of $F_{A,B}$ present. However, complete removal of $F_{A,B}$ does not lead to a complete loss of the nanosecond phase but reduces its amplitude by more than a factor of 2 to yield an amplitude of 25−30% relative to the initial picosecond rise, with only a slight change in kinetics. The residual amplitude is further reduced when a large fraction of F_X is removed. These results show that electron transfer from A_1 to F_X as well as from A_1 to $F_{A,B}$ is electrogenic. They support a model where F_X is an intermediate electron acceptor between A_1 and $F_{A,B}$ and suggest that the reduction of F_X is the rate-limiting process for the reduction of $F_{A,B}$. The relative amplitudes of the electrogenic phases allow an estimation of the dielectrically weighted transmembrane distances between the electron carriers in PS I. A_1 is found to be almost centrally positioned between A_0 and F_X. This structural information is compared to the structure emerging from X-ray crystallography.

The reaction center (RC)[1] of photosystem I in oxygen-evolving organisms contains three iron−sulfur centers (F_X, F_A, F_B) as terminal membrane-bound electron acceptors. The redox midpoint potential of F_A and F_B is sufficiently low to reduce $NADP^+$ via soluble ferredoxin. Two further electron acceptors mediate electron transfer from the primary donor (P700) to the Fe−S centers, a chlorophyll *a* functioning as the primary acceptor (A_0) and a quinone molecule (vitamin K_1) as the secondary acceptor (A_1). Recently, the structure of PS I from *Synechococcus* was determined by X-ray crystallography at 6-Å resolution (Krauss et al., 1993). This allowed the position of the three Fe−S centers, but not of the earlier acceptors A_0 and A_1, to be identified [see Golbeck (1993a) for a review on the structure of PS I]. Thus, up to now detailed structural information, as it exists for RCs of purple bacteria, has not been available for PS I.

Considerable experimental work on the electron transfer reactions in PS I has been performed [for a review, see Golbeck (1992)]. There is now wide agreement on the nature of the electron carriers involved, but there is still much uncertainty about the reaction pathways and about the role of some redox centers under physiological conditions. Especially concerned are redox reactions involving the three Fe−S centers, which are difficult to study by absorption spectroscopy due to their very weak optical absorption and the similarity of their optical spectra. In view of the experimental difficulties in distinguishing kinetically F_A and F_B, these two centers are frequently referred to as $F_{A,B}$. Information about these Fe−S centers relies largely on EPR data obtained at cryogenic temperatures.

As a basic principle in all photosynthetic RCs, light excitation induces charge separation within the transmembrane protein. An electron is transferred across the photosynthetic membrane, thereby building up a membrane potential. This potential difference can be detected by macroscopic electrodes. Each electron transfer step, involving a component perpendicular to the plane of the membrane, is called electrogenic and contributes to the potential. Time-resolved photoelectric techniques are a selective and sensitive tool to study the kinetics of electrogenic reactions. In addition, as the amplitudes of the photovoltage are related to the dielectrically weighted transmembrane distances beween the cofactors, direct electric measurements give important structural information.

The primary photochemistry in photosynthetic RCs involves a series of forward electron transfer reactions which, in general, become slower as the electron is stepwise removed from the primary donor. The primary event of

* Author to whom correspondence should be addressed. E-mail: Leibl@DSVIDF.CEA.FR.

[⊗] Abstract published in *Advance ACS Abstracts,* July 15, 1995.

[1] Abbreviations: A_0, A_1, primary (chlorophyll *a* monomer), secondary (phylloquinone) acceptor of photosystem I; DCPIP, 2,6-dichlorophenolindophenol; Fe−S center, iron−sulfur center; F_X, F_A, and F_B, the [4Fe−4S] centers of photosystem I; MES, 2-(*N*-morpholino)-ethanesulfonic acid; P700, primary donor of photosystem I; PMS, phenazine methosulfate; PS I, photosystem I; RC, reaction center.

0006-2960/95/0434-10237$09.00/0

PS I electron transfer is charge separation between the excited state of the primary donor P700* and the primary electron acceptor A_o forming the primary radical pair $P700^+/A_o^-$. This occurs on a time scale of several picoseconds (Hastings et al., 1994; Holzwarth et al., 1993; Kumazaki et al., 1994). In all photosynthetic RCs, a second electron transfer step leads to stabilization of the negative charge on a quinone acceptor (A_1 in PS I) within 1 ns. Picosecond photovoltage measurements have successfully been applied to study the fast reactions in the photosystems of plants and photosynthetic bacteria (Deprez et al., 1986; Leibl et al., 1989; Hecks et al., 1994). In order to achieve a picosecond time resolution, the photovoltage technique was based on a microcoaxial measuring cell connected to electrical devices with 50 Ω input impedance. However, as a consequence of the limited source capacitance of the microcoaxial cell (~30 pF), the photovoltage signals recorded show a RC decay of 1−2 ns, thus preventing the detection of subsequent slower reactions.

To overcome this limitation, high-input impedance amplifiers can be used. This opens up a time window from 1 ns to ~50 ns, the decay now being determined by the internal resistance (ionic conductivity) of the sample. Using these techniques, Trissl and co-workers came to the conclusion that there was no further detectable electrogenic phase up to 50 ns in PS I (Trissl et al., 1987). These early experiments were done with chloroplasts using the light-gradient technique with the implication of a poor signal-to-noise ratio due to the detection of small difference signals. A much better signal-noise ratio can be achieved with oriented membrane sheets, where, in the ideal case, the signal is the sum of the contributions of all individual membranes in an ordered stack.

Measurements using this photoelectric technique, on stacked oriented membranes, for reactions slower than ~50 ns have not been reported so far. Other systems based on a monolayer adsorbed to a high-ohmic support such as Teflon (Trissl et al., 1977) or phospholipid-impregnated collodion (Drachev et al., 1978) seem better adapted for the measurement of photovoltage kinetics on the microsecond to millisecond time scale. However, there are several advantages of using oriented membranes in the microcoaxial cell: orientation of the membranes by an electric field pulse is fast and easy to achieve as the same two electrodes of the capacitative cell can be used for both orientation and detection of the photoresponse, large signals are obtained due to the stacking of the membranes, the degree of asymmetry (orientation) is usually high, and access to a fast (picosecond) time scale using the same sample is possible. These reasons led us to try to use this technique for the investigation of further electrogenic reactions on a slower (nanosecond) time scale.

In this work we have applied photoelectric techniques to study electron transfer to the Fe−S centers in PS I. One of the points addressed concerns the position of the quinone acceptor A_1 with respect to F_X. F_X bridges the two large subunits of the heterodimeric core complex in a way that has been compared to the role of the non-heme iron of the RC of purple bacteria (Golbeck, 1988; Nitschke & Rutherford, 1991). Information about the transmembrane distance between A_1 and F_X will therefore show how strong the structural analogy is between the different types of RCs.

EXPERIMENTAL PROCEDURES

Sample Preparation. *Synechocystis* PCC 6803 was grown in BG 11 liquid media. The cells were harvested in the late logarithmic growth phase, and PS I particles were prepared as described elsewhere (Bottin & Sétif, 1991). The PS I membranes were stored until use at −80 °C in the presence of 20% glycerol and at a chlorophyll concentration of 2 mg/mL. Extraction of F_A and F_B was performed by urea treatment as described (Golbeck et al., 1988): the PS I membranes were incubated in 6.8 M urea for the time stated and then washed with 2 mM Mes pH 6.0. Removal of F_X was performed according to Warren et al. (1993): the $F_{A,B}$-extracted sample was incubated for 3 h in 3 M urea and 5 mM ferricyanide. The removal of $F_{A,B}$ and F_X was monitored by flash-induced absorption changes at 820 nm. At this wavelength, the flash-induced oxidation of P700 and its rereduction by backreaction with the terminal acceptor is detected. Ordinarily, the kinetics at 820 nm was measured from the nanosecond to the second time range. This allowed us to quantify a possible heterogeneity in acceptor population introduced by the biochemical treatment. In some cases, the kinetics of A_1^- reoxidation was measured by absorption spectroscopy at 380 nm (Brettel, 1988) to detect possible changes in the kinetics upon extraction of $F_{A,B}$ or to quantify the amount of F_X present. Before measurements, all samples were washed in 2 mM MES (pH 6) to reduce the ionic strength to a level that allows orientation of the membranes in a weak electric field.

Photoelectric Measurements. Photoelectric measurements were carried out on oriented membrane fragments in a microcoaxial measuring cell as described earlier (Trissl et al., 1987). Orientation was achieved by applying a short voltage pulse to the electrodes (10 V for ~100 ms). Using this orientation procedure, the membranes sediment electrophoretically onto the platinum electrode (anode), forming a stable multilayer which allows exchange of the buffer solution with virtually no loss of orientation. Unless stated otherwise, the oriented membranes were overlaid with 2 mM MES pH 6.5, 5 mM ascorbate, and 100 μM PMS. Excitation of the sample was by a Q-switched Nd/YAG laser (Quantel, France; wavelength, 532 nm; duration, 7 ns; pulse energy, ~2 mJ/cm^2). The flashes were applied to the measuring cell via a bifurcated light guide, by which white background light from a projector lamp could also be applied. Signals were recorded on a 100-MHz digital storage oscilloscope (Tektronix 2232) either after 10-fold amplification by broad-band preamplifiers with high input impedance (Model EMV80, M&S Elektronik; Model DA-20, Phoenicon) or after passing through a current-to-voltage amplifier (Model IU 502D, Phoenicon). The coaxial measuring cell was connected directly to the input connector of the amplifiers to minimize the external stray capacitance and to avoid distortions of the signal due to reflections. All measurements were done at room temperature.

Spectroscopic Measurements. Flash-induced absorption changes at room temperature were measured at 820 nm using a laser diode (SDL-5411-G1 from Spectra Diode Labs) as source of the measuring light and a photodiode (FND 100 from EG&G) as the detector. For excitation, a frequency-doubled Nd/YAG laser (Quantel, France: wavelength, 532 nm; duration, 300 ps; pulse energy, ~2 mJ/cm^2; repetition rate, 0.1 or 1 Hz) was used. Signals were recorded on a digitizing signal analyzer (Tektronix DSA 602A). A cuvette (1-cm optical path length) contained the sample at a chlorophyll concentration of ~10 μM. Ascorbate (2 mM) and DCPIP (100 μM) were added as slow external donors to P700. A ratio of 70 Chl/P700 was estimated from the

absorption change at 820 nm, assuming an absorption coefficient of 6500 M^{-1} cm^{-1} for $P700^+$ (Mathis & Sétif, 1981). For absorption change measurements at 380 nm, a xenon flash and a quartz curvette (2 mm) was used. The time resolution of the setup for absorption change measurements was ~5 (820 nm) or 10 ns (380 nm).

Data Analysis. Absorption kinetics were fitted to a multiexponential decay using a least-squares algorithm. The analysis of the photovoltage kinetics was based on a consecutive reaction scheme with two or three first-order reaction steps describing the molecular electron transfer processes. Under ideal open circuit conditions, the resulting displacement current is perfectly integrated by the capacitative measuring cell to yield the corresponding photovoltage (Deprez et al., 1986). Under real conditions, the photovoltage signal decays due to the discharge of the cell capacitance into the input impedance of the amplifier or internally due to the conductivity of the sample (see Results). For analysis of the photovoltage kinetics, this RC decay was taken into account by performing a convolution of the displacement current with the apparatus response function. The latter is given by an exponential decay and a Gaussian function which describes the time resolution of the setup. An alternative approach is to calculate an ideal photovoltage as the integral of the displacement current and to compare it to experimental traces where the RC decay has been removed by a numerical deconvolution procedure (such traces are referred to in the following as "decay-cleared" experimental traces).[2] A fit procedure based on a least-squares algorithm was used to determine the parameters (time constants and electrogenicity factors) of the calculated photovoltage response which optimally match the kinetics of the experimental traces.

RESULTS

The photoelectric response of oriented PS I membranes excited with 7-ns flashes is shown in Figure 1a,b. Both traces were recorded under identical conditions except that samples in panel b contained 66% (v/v) glycerol, thereby altering the ionic strength and the viscosity of the environment. After recording of trace a, the oriented membranes were covered with 66% (v/v) glycerol and equilibrated for some minutes, and then trace b was recorded. Both traces show a fast rise which is limited by the rise time of the amplifier used in this experiment (35 ns). This fast phase contains the two first steps of charge separation occurring within 100 ps. These steps are not time-resolved here but have been characterized previously with a picosecond system (Hecks et al., 1994). A comparison of the data in Figure 1 a and b shows that in the absence of glycerol (Figure 1a) the photovoltage signal decays with a $\tau_{1/e}$ of ~50 ns due to ionic relaxations within the sample. When the viscosity of the solution is increased (Figure 1b), the decay is significantly slower due to the strongly reduced conductivity of the sample, and under these conditions, an additional slow electrogenic phase is clearly visible. Careful analysis of the traces without glycerol (Figure 1a) shows that a comparable additional slow phase is indeed present but is masked by the fast decay. This is demonstrated by the residual plots (lower traces in Figure 1a) resulting from a fit of the experimental trace. The analysis shows that the kinetics cannot be described by a single-exponential decay. An additional slow phase similar to the one visible in the presence of glycerol has to be taken into account to simulate

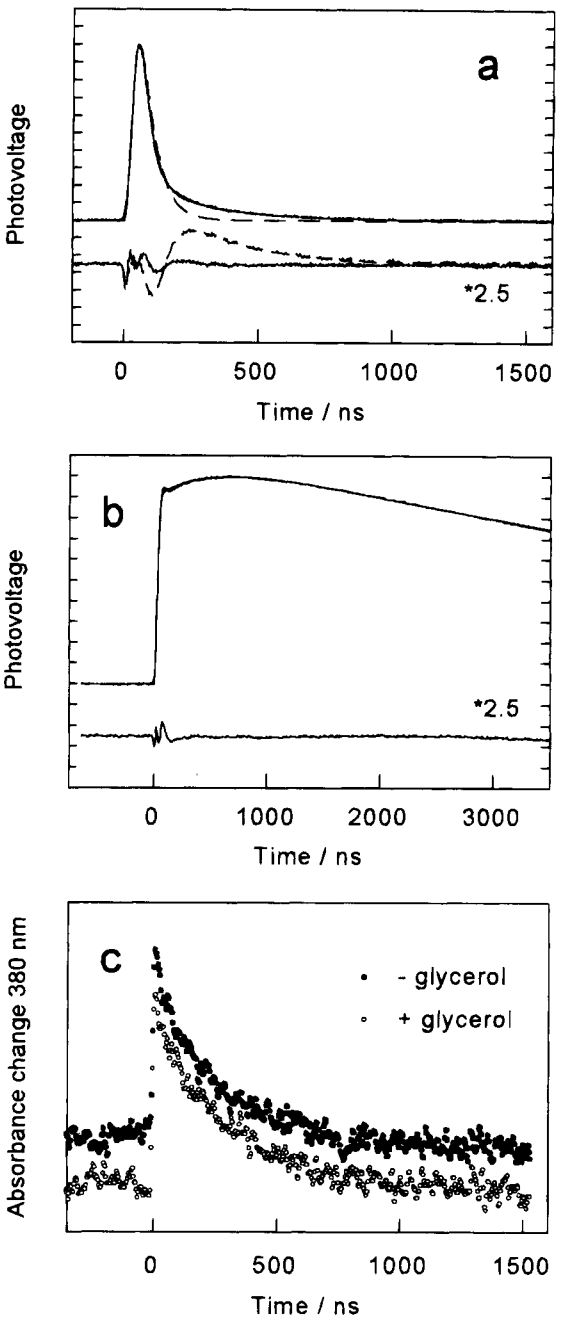

FIGURE 1: Photovoltage of irreversibly oriented PS I membranes excited with 7-ns flashes in the presence of 5 mM ascorbate and 100 μM PMS. Experimental and calculated traces are shown superimposed. (a) Photovoltage kinetics of samples in 2 mM Mes buffer pH 6.5. Solid lines: best fit according to a biphasic electrogenic reaction (τ_1 < 1 ns, τ_2 = 233 ns, relative amplitudes a_1/a_2 = 1:0.68). Dashed lines: best fit according to a monophasic electrogenic reaction. (b) Photovoltage kinetics in the presence of 66% (v/v) glycerol. Differences between experimental and calculated traces are shown as residuals below (multiplied by a factor of 2.5). The time resolution was 35 ns, limited by the electrometer amplifier. (c) Absorbance change kinetics at 380 nm in the absence and presence of 66% glycerol. In both samples, 2 mM Mes, pH 6.5, 5 mM ascorbate, and 400 μM DCPIP were present.

[2] Let $C(t)$ be the displacement current induced in the sample and $V(t)$ the experimentally measured photovoltage. The relationship between $C(t)$ and $V(t)$ in an ideal system is $V(t) = \int_0^t C(t)\,dt$. An exponential decay with a rate constant k_d in the system response function (low-frequency roll-off) is described by the convolution equation $V(t) = \int_0^t C(x)\exp[-k_d(t - x)]\,dx$. This equation can easily be solved for $C(t)$ yielding $C(t) = k_d V(t) + d/dt V(t)$ and by integration the deconvoluted (decay-cleared) photovoltage $V'(t) = \int C(t)\,dt = V(t) + k_d \int V(t)\,dt$.

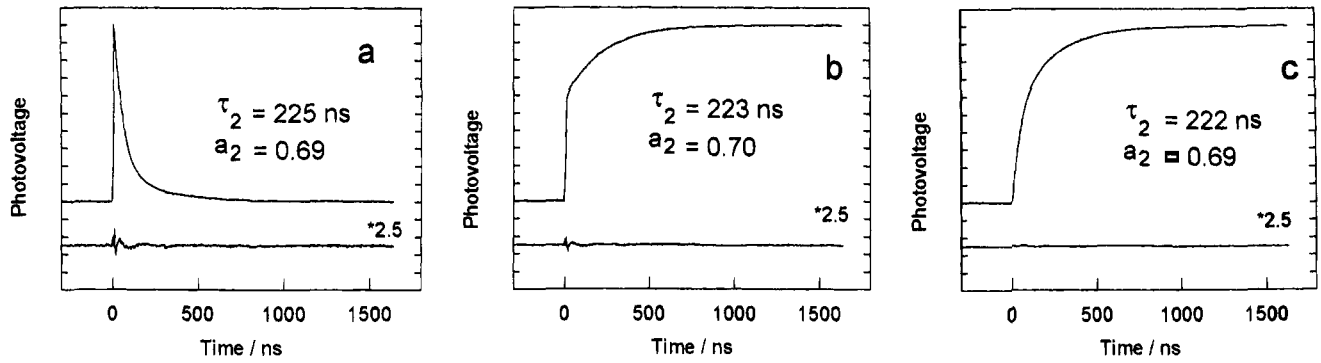

FIGURE 2: Photovoltage kinetics from PS I membranes. Conditions as in Figure 1a except amplifier (R_i = 20 kΩ; rise time, 5 ns): (a) original experimental trace, (b) "decay-cleared" experimental trace, and (c) numerically integrated experimental trace. The kinetics were analyzed by a fit of theoretical traces calculated (a) as the convolution of the biphasic displacement current with the exponential decay, (b) as an ideal biphasic photovoltage, and (c) as an ideal biphasic photovoltage with limited fast rise. See text for details of calculation. For clarity, calculated traces are not shown superimposed but the deviations are shown as residual plots below the traces (multiplied by a factor of 2.5). Parameters obtained from the best fits are stated in the figures. The time constant for the ionic decay was 46 ns.

the experimental traces. It is important to realize that under conditions of relatively high conductivity (fast discharge), the system characteristics are determined as approximately voltage clamped. This corresponds more to a photocurrent measurement. As, in general, in a capacitative system, the photovoltage results from an integration of a photocurrent, both contain the same information [for a review on photoelectric measurements, see Trissl (1990)]. However, the amplitudes in the photocurrent measurement are weighted with the rate constants of the reaction, which leads to small amplitudes of the slow phases. To obtain the electrogenicity factor of a given reaction step from a photocurrent trace, a correct analysis of the kinetics is therefore necessary.

As demonstrated in Figure 2, there are slightly different ways to analyze the measured kinetic traces like the one in Figure 1b, depending on the data being considered as photovoltage with a fast decay or photocurrent with limited time resolution. In the first case, the displacement current is calculated according to a presumed reaction scheme and convoluted with an exponential decay and the result fit directly to the original data (Figure 2a). Alternatively, a "decay-cleared" photovoltage (see Experimental Procedures) can be obtained by appropriate deconvolution to which a calculated photovoltage (integrated displacement current) can be fit (Figure 2b). In the second case, the data can be integrated numerically to yield the corresponding photovoltage, which is compared to a calculated photovoltage (Figure 2c). It is notable that the fast rise time of the integrated trace is limited and shows the same kinetics as the ionic decay apparent in the original experimental trace. All three analysis procedures should yield identical results. That this is in fact the case is shown by the agreement between the parameters determined from the same experimental trace by the different approaches (Figure 2). However, the three methods exhibit different sensitivity to noise in the data. For example, it is obvious that the high-frequency noise is considerably reduced in the integrated traces (Figure 2c). For clarity of demonstration, the traces below will be presented "decay cleared" as in Figure 2b. This allows the best visual estimation of the relative amplitude of a slower electrogenic phase. Note that the trace in Figure 2 and those presented in the following were recorded with a higher time resolution (5−7 ns) than the traces in Figure 1.

The experiments were repeated with different ionic strengths of the sample solution and with amplifiers having different input impedance. The fact that these changes modified only the rate of the fast decay but not of the additional slow phase allowed us to exclude the possibility that the slow phase is an artifact of the electrical detection system. As a further control, the photocurrent was measured using a current-to-voltage converter which can sink the input current into virtual ground (Bard & Faulkner, 1980). Within the limit of accuracy, this measurement gives the same results for the kinetics and amplitude of the electrogenic phases (not shown). Kinetic analysis of a large number of experiments gave for the slow electrogenic phase a relative amplitude of 0.66 ± 0.10 as compared to the amplitude of the unresolved faster phases (which were normalized to 1) and an exponential time constant of $\tau_{1/e}$ = 220 ± 20 ns.

The kinetics of the slow electrogenic phase agree well with the reoxidation kinetics of A_1^- measured by absorption spectroscopy and time-resolved EPR in PS I of cyanobacteria (Brettel, 1988; Bock et al., 1989; van der Est et al., 1994). Therefore the assignment of the electrogenic 220-ns phase to electron transfer from A_1 to the Fe−S centers as further electron acceptors seems a reasonable hypothesis. As a control, the reoxidation kinetics of A_1^- in the sample used for the photoelectric experiments were measured by the flash-induced absorbance changes at 380 nm (Figure 1c). The kinetics are well described with one exponential time constant of 200−230 ns and are only slightly slower in the presence of 66% glycerol. There is a good agreement between the absorbance change kinetics and the kinetics of the slow electrogenic phase observed without glycerol. However, in the presence of glycerol the kinetics of the electrogenic phase appeared significantly slower (350−600 ns, depending on the glycerol concentration) and the amplitudes smaller (0.25−0.45) than in the absence of glycerol. As will be discussed below, this could be due to an effect of glycerol on the dielectric relaxation properties of the medium around $F_{A,B}$ rather than to an effect on the kinetics of A_1^- reoxidation. Alternatively, glycerol might change the electrical response of the measuring cell in the photovoltage experiment, a possibility that cannot totally be excluded at present. For these reasons, the data presented in the following were obtained without glycerol, which also corresponds to more physiological conditions and allows a better control of pH and redox conditions.

Electron transfer to the iron−sulfur centers is blocked when these acceptors are already reduced before the flash. In Figure 3 are shown the photovoltage kinetics under strongly reducing conditions. After addition of dithionite

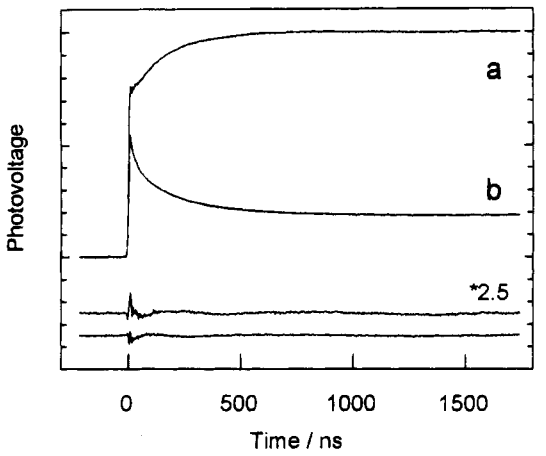

FIGURE 3: Photovoltage kinetics from PS I membranes under strongly reducing conditions (10 mM dithionite and 10 mM glycine pH 10) (a) without and (b) with background illumination. Traces were analyzed after deconvolution of the ionic decay, which was assumed to be identical for both traces. Calculated traces are not shown superimposed, but deviations are shown as residual plots on the bottom. Parameters obtained from best fits: (a) $\tau_2 = 170$ ns, $a_2 = 42\%$; (b) $\tau_2 = 26$ ns, $a_2 = -34\%$, $\tau_3 = 230$ ns, $a_3 = -36\%$. The time constant for the ionic decay was 34 ns for both traces.

to the oriented sample, a 220-ns phase was still detected (Figure 3a), although its amplitude was decreased. When background light was applied, the slow positive phase was lost and negative phases with kinetics of about 25 and 230 ns appeared (Figure 3b). $F_{A,B}$ can be (partially) reduced chemically at high pH whereas F_X^- can only be photoaccumulated (Rutherford & Heathcote, 1985). Therefore, we interpret the positive 220-ns phase as being the reduction of Fe−S centers by A_1. On photoaccumulation of all Fe−S centers to the reduced state this phase is replaced by fast backreactions between $P700^+$ and a preceding acceptor [$P700^+ A_1^- Fe-S^- \rightarrow P700 A_1 Fe-S^-$; $\tau = 250$ ns (Sétif & Brettel, 1990); or $P700^+ A_o^- A_1^- \rightarrow P700 A_o A_1^-$; $\tau = 25$ ns (Warren et al., 1993)]. It has previously been shown that A_o and A_1 are located before F_x (Sétif & Bottin, 1989; Bottin & Sétif, 1991).

If the 220-ns phase is related to electron transfer to the Fe−S centers it should be affected not only by the (photo)-chemical reduction but also by the removal of these Fe−S centers. To test this hypothesis and to characterize further the electrogenic reaction, we studied the effect of urea treatment. This treatment has been shown to result in removal of the extrinsic polypeptide PSI−C, which carries F_A and F_B (Golbeck et al., 1988). PS I membranes were incubated in 6.8 M urea and samples were taken at different incubation times. In the following, all samples were treated exactly the same way. The samples were washed several times in 2 mM Mes buffer and then used for parallel measurements of both the photovoltage and the absorbance changes. The kinetics of $P700^+$ rereduction were monitored by measuring absorbance changes at 820 nm following laser flash illumination. This quantified the remaining fraction of $F_{A,B}$, based on the characteristic $\tau_{1/2}$ of backreaction between either $P700^+$ and $F_{A,B}^-$ (30−100 ms) or $P700^+$ and F_X^- (0.6−1 ms). The kinetics of absorption change at 820 nm were measured also in the submicrosecond and microsecond range to check for eventual damage of acceptor sites preceding $F_{A,B}$. The effect of the urea treatment is shown in Figure 4. The absorbance change measurements demonstrate that the slow decay of $P700^+ F_{A,B}^-$ (50 ms) is progressively replaced by a faster decay with a time constant of ~0.7 ms as the incubation time is increased (Figure 4b). In this particular experiment, 50% of $F_{A,B}$ had been removed after ~20 min of incubation. Only in the most extensively treated sample, a small phase with a time constant of ~15 μs was observed, indicating that 15% of F_X had been lost. The photoelectric measurements clearly show that the urea treatment leads to a decrease of the amplitude of the 220-ns phase (Figure 4a). The kinetics are virtually unchanged except for a small acceleration on the most extensively treated sample ($\tau = 180$ ns). When the relative amplitude of the 220-ns phase is plotted versus the fraction of reaction centers with intact $F_{A,B}$, a clear correlation is observed (Figure 4c). A linear regression analysis indicates a relative amplitude of the 220-ns phase of 0.66 ± 0.1 in the intact system and of 0.27 ± 0.03 in the $F_{A,B}$-depleted system.

The electrogenic phase remaining after complete depletion of $F_{A,B}$ is most easily attributed to electron transfer from A_1 to F_X. To verify this attribution, we tried to remove F_X by oxidative denaturation (Warren et al., 1990). This preparation is difficult to handle as, in the absence of F_X, the phylloquinone A_1 is easily lost, resulting in a significant fraction of fast backreaction kinetics (20−40 ns) in both the 820-nm absorption changes and the photovoltage measurements. It was found that the loss of A_1 could be avoided when the extraction of F_X was performed in the presence of excess vitamin K1. In this case, however, the test for the degree of extraction of F_X by measuring the backreaction kinetics at 820 nm is difficult, as vitamin K_1 might function as external electron acceptor in the microsecond to millisecond time range. Therefore, we used the reoxidation kinetics of A_1^-, measured at 380 nm, as another indicator for the presence of F_X (data not shown). Upon removal of F_X, the 200-ns phase of the absorbance change is decreased and A_1^- is stable on the submicrosecond time scale. The most thoroughly extracted sample that exhibits no detectable nanosecond backreaction contained ~50% of F_X. In this preparation, the relative amplitude of the slow electrogenic phase is decreased to 10−15% of the amplitude of the subnanosecond phase and its kinetics appear also somewhat accelerated compared to the intact sample. The trace-designated "50% F_X" in Figure 4a represents an example. This parallel decrease of the amplitude of the 220-ns phase and of the amount of F_X is consistent with our assignment of the 220-ns phase remaining after removal of $F_{A,B}$ to electron transfer from A_1 to F_X.

DISCUSSION

A recent study of the picosecond photovoltage on oriented PS I membranes from *Synechocystis* sp. PCC 6803 with high time resolution has revealed two steps of charge separation occurring within 100 ps (Hecks et al., 1994). The first step (22 ± 4 ps) was attributed to the primary charge separation $P^+A_o^-$) and the second one (50 ± 15 ps) to subsequent electron transfer to A_1. Assuming a homogeneous dielectric in the RC core, the relative amplitude of both phases (1: 0.25 ± 0.13) was interpreted as the ratio of the transmembrane distances P700−A_o and A_o−A_1.

The extension of these photoelectric measurements to the nanosecond time range presented in this work reveals a third electrogenic phase. This phase is sensitive to the presence and the redox state of the Fe−S centers and its kinetics correspond to the kinetics of reoxidation of A_1^- as measured

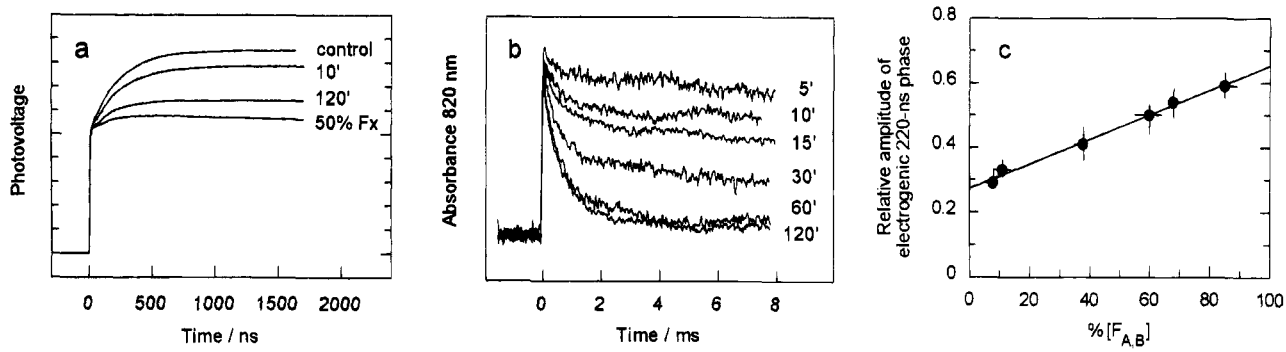

FIGURE 4: (a) Photovoltage of PS I membranes after urea treatment to selectively remove Fe−S centers: (control) control, (10′) 10 min urea treatment, (120′) 120 min urea treatment, and (50% F_X) 3 h urea/ferricyanide treatment in the presence of excess vitamin K_1. The traces were normalized according to the relative amplitude of the 220-ns phase (a_2) as determined by the best fit. This results in a maximum amplitude proportional to $(1 + a_2)$ and a matching of the amplitude of the unresolved fast rise. Fit parameters: (control) $\tau_2 = 223$ ns, $a_2 = 0.70$; (10′) $\tau_2 = 236$ ns, $a_2 = 0.57$; (120′) $\tau_2 = 176$ ns, $a_2 = 0.28$; (50% F_X) $\tau_2 = 167$ ns, $a_2 = 0.15$. In the 50% F_X trace, a partial decay due to the backreaction between $P700^+$ and A_1^- ($\tau \approx 15$ μs) is visible. (b) Calibration of $[F_{A,B}]$ by analysis of the kinetics of flash-induced absorption changes at 820 nm (backreaction of 30−100 and 0.6−1 ms, respectively, in the presence and absence of $F_{A,B}$). (c) Correlation between the relative amplitude of the 220-ns phase of the photovoltage and the fraction of reaction centers with intact $F_{A,B}$. Gradual extraction of Fe−S centers was performed by urea treatment for different incubation times. Error bars indicate the variation due to the analysis of different experiments and due to different methods of analysis (see Figure 2). The straight line results from a regression analysis of the data yielding values of 0.27 and 0.0038 for the intercept and the gradient, respectively.

by the absorbance change kinetics at 380 nm. The kinetics of 220 ± 20 ns determined in this work are in good agreement with published results on the reoxidation of A_1^- in cyanobacteria (Brettel, 1988; Bock et al., 1989). The 220-ns phase can therefore be securely attributed to forward electron transfer from the phylloquinone acceptor A_1 to one of the Fe−S centers.

Preliminary experiments showed that the amplitude of the 220-ns phase was diminished after incubation of the PS I membranes in 6.8 M urea, a treatment that leads to removal of F_A and F_B (Warren et al., 1990). These biochemical procedures bear the risk of leading to a heterogeneity of the sample in terms of acceptor population. For example, it is difficult to obtain a preparation that keeps all F_X when $F_{A,B}$ is quantitatively removed. Therefore, a gradual extraction of $F_{A,B}$ was performed with the idea of increasing the precision of the measurement by extrapolating the relative amplitude of the 220-ns phase to $[F_{A,B}] = 0$. These experiments indicate that the relative amplitude of the slow electrogenic phase diminishes from 0.66 to 0.27 upon complete extraction of $F_{A,B}$, with little effect on the kinetics. The fact that in the absence of $F_{A,B}$ a significant fraction of the slow phase is still observed shows that under these conditions electron transfer from A_1 to F_X occurs and that this transfer is electrogenic although its electrogenicity is less than half that of electron transfer from A_1 to $F_{A,B}$ in the intact system. It further shows that the kinetics of electron transfer from A_1 to F_X in the $F_{A,B}$-depleted system is very similar to the kinetics of electron transfer from A_1 to $F_{A,B}$ in the intact system. The similarity of the kinetics in the presence or the absence of $F_{A,B}$ is taken as evidence that F_X functions as intermediate electron acceptor in the intact system. This result is in accordance with conclusions drawn from spectroscopic measurements of A_1^- reoxidation kinetics in native and $F_{A,B}$-depleted samples from *Synechococcus* and *Synechocystis* (Moënne-Loccoz et al., 1994; Lüneberg et al., 1994; van der Est et al., 1994). A slight difference in the kinetics of electron transfer from A_1 to F_X in the presence and absence of the extrinsic polypeptide carrying $F_{A,B}$ can be explained by a modification of the environment of F_X. The latter is likely to be more polar in the absence of $F_{A,B}$ stabilizing the reduced state of F_X. The removal of $F_{A,B}$ is not equivalent to the reduction of $F_{A,B}$. It has been shown that, after reduction of $F_{A,B}$, the electron transfer from A_1 to F_X is inhibited. This has been explained by an electrostatic effect (Brettel, 1989; Sétif & Brettel, 1993) and is therefore not an argument against F_X functioning as acceptor in the native electron transfer chain.

The result of the effect of biochemical treatment on the relative amplitude of the slow electrogenic phase relies on the assumption that the sample treatment does not cause a drastic change in the kinetics, converting part of the 220-ns phase into either a much faster or a much slower phase which could escape detection. There are reports of a biphasic reoxidation kinetics of A_1^- with a second phase of $\tau_{1/e} = 36$ ns the relative amplitude of which depends on the species and the preparation procedure (Sétif & Brettel, 1993; van der Est et al., 1994). This phase was interpreted as fast electron transfer to F_X in part of the RCs (Sétif & Brettel, 1993). We have observed a similar phase in the absorbance kinetics at 380 nm in *Synechocystis* samples which were treated with urea for a time longer than necessary to completly remove $F_{A,B}$. Less treated samples showed no significant fraction of fast absorbance kinetics at 380 nm. The analysis of the photoelectrical data would detect a 35-ns phase with significant electrogenicity, and such phases have been indeed observed in photoelectric measurements on PS I particles from spinach (unpublished results). In general, PS I preparations from *Synechocystis* show a much smaller relative amplitude of the 35-ns phase (<15%) than preparations from spinach (Sétif & Brettel, 1993; van der Est et al., 1994). In conclusion, the measurements in this work show that in samples still having all F_X intact contributions from a possible 35-ns phase must be small and the loss of amplitude of the 220-ns phase upon urea treatment (Figure 4) cannot be explained by conversion into a 35-ns phase. It is estimated that the error introduced into the analysis by a small portion of centers with fast $A_1 \rightarrow F_X$ electron transfer, which could be present in the more thoroughly treated samples, falls within the error bars given.

Kinetic EPR and absorbance change measurements detect essentially the reoxidation of A_1^- and therefore can follow the electron transfer only to F_X. The photovoltage measurements are sensitive to further transfer to $F_{A,B}$ as shown by

the ~2 times larger amplitude of the 220-ns phase in the presence of $F_{A,B}$. The results in this work demonstrate that the reduction kinetics are very similar for F_X and $F_{A,B}$. This leads us to propose that electron transfer from A_1 to F_X is the rate-limiting process for reduction of $F_{A,B}$, i.e., that the intrinsic time constant for electron transfer from F_X to $F_{A,B}$ is faster than 220 ns. Recently, a 500-ns phase was attributed to reduction of ferredoxin (Sétif & Bottin, 1994). According to these authors, ferredoxin is not likely to be reduced directly by F_X as the estimated distance between F_X and ferredoxin is too large. Therefore, the fast phase of ferredoxin reduction is another indication for a fast (submicrosecond) electron transfer from F_X to the next electron acceptor, F_A or F_B. Submicrosecond electron transfer kinetics between $F_{A,B}$ and ferredoxin are compatible with the binding geometry proposed for these acceptors (Sétif & Bottin, 1994).

The photoelectric study presented in this work leads to a reaction scheme where electron transfer from A_1 to F_X is relatively slow (220 ± 20 ns) and exhibits an electrogenicity only slightly smaller than that of the following step of electron transfer from F_X to $F_{A,B}$. If the rate constant for electron transfer from F_X to $F_{A,B}$ is greater than the rate constant for electron transfer from A_1 to F_X, a sigmoidicity of the photovoltage kinetics is expected. The degree of sigmoidicity depends on the rate of the second, faster step. Close inspection of the photovoltage kinetics measured in the intact system gives some indication for a second kinetic phase with a time constant of ~15 ns. However, the response of the amplifiers used in this work is not sufficiently flat in the first 50 ns after the fast rise to allow a precise analysis in this time domain. It should also be noted that the sigmoidicity of the photovoltage kinetics is expected to be less pronounced than the sigmoidicity in the time-dependent concentration of the state $[F_{A,B}^-]$ because of the significant electrogenicity of the $A_1 \rightarrow F_X$ electron transfer step. Therefore, an estimation of the kinetics of $F_X \rightarrow F_{A,B}$ electron transfer cannot be made from the present data. They only allow us to give an upper limit of ~50 ns for the time constant of this reaction.

The fact that electron transfer from A_1 to $F_{A,B}$ occurs in two consecutive steps invites to speculate about a possible explanation for the effect of glycerol on the photovoltage kinetics (Figure 1). In the presence of glycerol, the apparent kinetics of the slow electrogenic phase are slower and its apparent amplitude is smaller whereas the absorbance change measurements show that the reoxidation kinetics of A_1^- are hardly affected. However, the slow phase of the photovoltage contains not only the electron transfer step from A_1 to F_X but also the following step of electron transfer from F_X to $F_{A,B}$, which contributes even slightly more. As pointed out above, the analysis of the slow phase with a single exponential is only correct if the second step is much faster than the first one. Although this condition seems fulfilled in the absence of glycerol, this might not be the case in the presence of glycerol. In fact, the slow phase of the photovoltage in the presence of glycerol can perfectly be described by a two-step reaction with the parameters of the first step as in the absence of glycerol (time constant of 220 ns and relative electrogenicity of 0.27) and a second step, the kinetics of which depend on the concentration of glycerol (100−800 ns). An effect of glycerol on the redox midpoint potential of F_A and F_B has been reported (Evans & Heathcote, 1980) but it is unclear whether electron transfer to F_B and F_A is affected or not (Bottin et al., 1987; Sakurai et al., 1991).

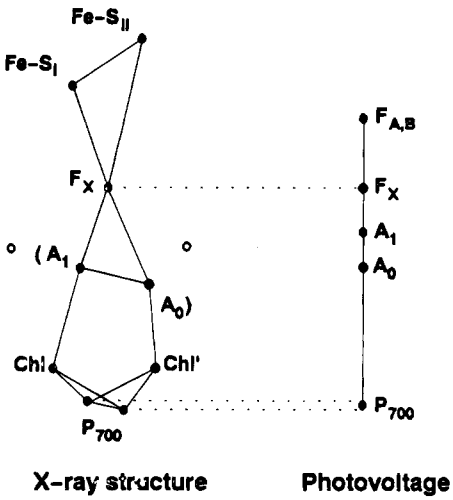

FIGURE 5: Comparison between the transmembrane location of redox components in PS I according to (a) the X-ray structure [adapted from Krauss et al. (1993)] and (b) photoelectric measurements [Hecks et al. (1994) and this work].

Before a statement about the possible molecular mechanism can be made, it is necessary to perform further experiments on the photovoltage kinetics as a function of the concentration of glycerol and of temperature to fully exclude a specific effect of the dielectric properties of a glycerol solution on the electrical detection system.

The dielectrically weighted transmembrane distances obtained by photoelectric measurements can be compared to the structural model emerging from X-ray crystallography (Krauss et al., 1993). At the present resolution of the X-ray data, the proposed locations of A_o and A_1 have to be taken with care while that of P700 and, even more so, of the Fe−S centers seem securely assigned. Therefore, in Figure 5 the photoelectric data have been normalized to the position of P700 and of F_X from the X-ray data. This allows the relative positions of the other cofactors to be compared. Taking into account the experimental error, the positions of A_o and A_1 compare well, although the results of the photovoltage experiments favor a position of the quinone acceptor A_1 which is more distant from A_o. This could correspond to the alternative location (open circles in Figure 5) for a quinone in the structure proposed by Krauss et al. (1993) as was already pointed out on the basis of the relative amplitudes of the photovoltage in the picosecond range (Hecks et al., 1994). In this respect, the results of the photovoltage on the picosecond and nanosecond time scale are fully compatible with the X-ray model, especially when the alternative location of A_1 is considered. The photovoltage results indicate fractional dielectrically weighted transmembrane distances of 0.62, 0.16, and 0.22 for P700−A_o, A_o−A_1, and A_1−F_X, respectively.

The X-ray structure indicates F_X to be located at the interface between the two chlorophyll-binding polypeptides psaA and psaB. This is similar to the central location of the non-heme iron in the RCs of purple bacteria with respect to the symmetrically arranged L and M protein subunits. In the RCs of purple bacteria, the quinone acceptors and the non-heme iron are located on the same level within the membrane. A position of A_1 and F_X on the same level relative to the membrane plane would strengthen the hypothesis of a common evolutionary origin of the different photosynthetic RCs. However, in this work a significant difference in the transmembrane location of A_1 and F_X is

found, supporting earlier models that F_X lies much closer to the surface of the membrane than does the non-heme iron in the purple bacterial RC (Golbeck, 1988; Nitschke & Rutherford, 1991). This indicates that the structural similarity between the two types of RCs, although present to a certain degree (Golbeck, 1993b; Nitschke & Rutherford, 1994), should not be taken too far.

Until now there is no clear attribution of the Fe−S centers F_A and F_B, as defined by EPR, to one of the two electron densities Fe−S_I and Fe−S_{II} appearing in the X-ray structure outside the membrane lipid layer (see Figure 5). The relative amplitude of the urea-sensitive electrogenic phase indicates a position close to Fe−S_I for the electron acceptor which is reduced by F_X. However, care should be taken in assigning the terminal electron acceptor seen in the photovoltage to this center. The photovoltage amplitude only indicates dielectrically weighted distances and therefore a direct interpretation in terms of relative distances is valid only for a homogeneous dielectric environment. This condition, probably fulfilled for the part of the RC that is inside the membrane protein/lipid layer, might not apply to the regions of the RC protruding out into the aqueous phase, where the effective dielectric constant might be higher. For such regions, significantly smaller photovoltage amplitudes are expected and are indeed observed (Dracheva et al., 1988). As F_A and F_B are located on an extrinsic polypeptide, the effective dielectric constant is probably higher than within the membrane. For this reason, the distance between F_X and the next acceptor, as apparent from photovoltage amplitudes, must be regarded as a lower limit. In particular, the photoelectric data presented above do not allow exclusion of the Fe−S cluster Fe−S_{II} as the terminal acceptor. Selective destruction of one of these two iron−sulfur centers might allow identification of F_A and F_B by further photoelectric experiments. Recently, an electrogenic phase with a kinetics of 30 ± 10 μs was measured in a PS I preparation from spinach and attributed to electron transfer from Fe−S_I to Fe−S_{II} (Sigfridsson et al., 1995). Although this attribution would appear compatible with the result of this work, further experiments are needed to show that the electron transfer reactions within the Fe−S acceptor complex in PS I from higher plants and cyanobacteria are comparable.

ACKNOWLEDGMENT

We thank Hervé Bottin, Klaus Brettel, and Pierre Sétif for helpful discussions, Dominique Dejonghe and Sandra Andrianambinintsoa for preparing PS I membranes, P. Brzezinski for communicating his manuscript prior to publication, and J. Hanley for critical and careful reading of the manuscript. We also thank Klaus Brettel for considerable assistance with the absorbance change measurements.

REFERENCES

Bard, A. J., & Faulkner, L. R. (1980) *Electrochemical Methods*, p 557, John Wiley & Sons, New York.

Bock, C. H., Van der Est, A. J., Brettel, K., & Stehlik, D. (1989) *FEBS Lett. 247*, 91−96.

Bottin, H., & Sétif, P. (1991) *Biochim. Biophys. Acta 1057*, 331−336.

Bottin, H., Sétif, P., & Mathis, P. (1987) *Biochim. Biophys. Acta 894*, 39−48.

Brettel, K. (1988) *FEBS Lett. 239*, 93−98.

Brettel, K. (1989) *Biochim. Biophys. Acta 976*, 246−249.

Deprez, J., Trissl, H. W., & Breton, J. (1986) *Proc. Natl. Acad. Sci. U.S.A. 83*, 1699−1703.

Drachev, L. A., Kaulen, A. D., & Skulachev, V. P. (1978) *FEBS Lett. 87*, 161−167.

Dracheva, S. M., Drachev, L. A., Konstantinov, A. A., Semenov, A. Y., Skulachev, V. P., Arutjunjan, A. M., Shuvalov, V. A., & Zaberezhnaya, S. M. (1988) *Eur. J. Biochem. 171*, 253−264.

Evans, M. C. W., & Heathcote, P. (1980) *Biochim. Biophys. Acta 590*, 89−96.

Golbeck, J. H. (1988) *Biochim. Biophys. Acta 895*, 167−204.

Golbeck, J. H. (1992) *Annu. Rev. Plant Physiol. Plant Mol. Biol. 43*, 293−324.

Golbeck, J. H. (1993a) *Curr. Opin. Struct. Biol. 3*, 508−514.

Golbeck, J. H. (1993b) *Proc. Natl. Acad. Sci. U.S.A. 90*, 1642−1646.

Golbeck, J. H., Parrett, K. G., Mehari, T., Jones, K. L., & Brand, J. J. (1988) *FEBS Lett. 228*, 268−272.

Hastings, G., Kleinherenbrink, F. A. M., Lin, S., McHugh, T. J., & Blankenship, R. E. (1994) *Biochemistry 33*, 3193−3200.

Hecks, B., Wulf, K., Breton, J., Leibl, W., & Trissl, H.-W. (1994) *Biochemistry 33*, 8619−8625.

Holzwarth, A. R., Schatz, G., Brock, H., & Bittersmann, E. (1993) *Biophys. J. 64*, 1813−1826.

Krauss, N., Hinrichs, W., Witt, I., Fromme, P., Pritzkow, W., Dauter, Z., Betzel, C., Wilson, K. S., Witt, H. T., & Saenger, W. (1993) *Nature 361*, 326−331.

Kumazaki, S., Kandori, H., Petec, H., Yoshihara, K., & Ikegami, I. (1994) *J. Phys. Chem. 98*, 10335−10342.

Leibl, W., Breton, J., Deprez, J., & Trissl, H.-W. (1989) *Photosynth. Res. 22*, 257−275.

Lüneberg, J., Fromme, P., Jekow, P., & Schlodder, E. (1994) *FEBS Lett. 338*, 197−202.

Mathis, P., & Sétif, P. (1981) *Isr. J. Chem. 21*, 316−320.

Moënne-Loccoz, P., Heathcote, P., Maclachlan, D. J., Berry, M. C., Davis, I. H., & Evans, M. C. W. (1994) *Biochemistry 33*, 10037−10042.

Nitschke, W., & Rutherford, A. W. (1991) *Trends Biochem. Sci. 16*, 241−245.

Nitschke, W., & Rutherford, A. W. (1994) in *Origin and Evolution of Biological Energy Conservation* (Baltscheffsky, M., Ed.) VCH Publishers, New York.

Rutherford, A. W., & Heathcote, P. (1985) *Photosynth. Res. 6*, 295−316.

Sakurai, H., Inoue, K., Fujii, T., & Mathis, P. (1991) *Photosynth. Res. 27*, 65−71.

Sétif, P., & Bottin, H. (1989) *Biochemistry 28*, 2689−2697.

Sétif, P., & Bottin, H. (1994) *Biochemistry 33*, 8495−8504.

Sétif, P., & Brettel, K. (1990) *Biochim. Biophys. Acta 1020*, 232−238.

Sétif, P., & Brettel, K. (1993) *Biochemistry 32*, 7846−7854.

Sigfridsson, K., Hansson, Ö., & Brzezinski, P. (1995) *Proc. Natl. Acad. Sci. U.S.A. 92*, 3458−3462.

Trissl, H.-W., Darszon, A., & Montal, M. (1977) *Proc. Natl. Acad. Sci. U.S.A. 74*, 207−210.

Trissl, H.-W., Leibl, W., Deprez, J., Dobek, A., & Breton, J. (1987) *Biochim. Biophys. Acta 893*, 320−332.

Trissl, H.-W. (1990) *Photochem. Photobiol. 51*, 793−818.

Van der Est, A., Bock, C., Golbeck, J., Brettel, K., Sétif, P., & Stehlik, D. (1994) *Biochemistry 33*, 11789−11797.

Warren, P. V., Parrett, K. G., Warden, J. T., & Golbeck, J. H. (1990) *Biochemistry 29*, 6545−6550.

Warren, P. V., Golbeck, J. H., & Warden, J. T. (1993) *Biochemistry 32*, 849−857.

BI943010J